Flow non-normality-induced transient growth in superposed Newtonian and non-Newtonian fluid layers

C. Camporeale,* F. Gatti, and L. Ridolfi
DITIC–Department of Hydraulics, Politecnico di Torino, Torino, Italy
(Received 25 May 2009; published 22 September 2009)

In recent years non-normality and transient growths have attracted much interest in fluid mechanics. Here, we investigate these topics with reference to the problem of interfacial instability in superposed Newtonian and non-Newtonian fluid layers. Under the hypothesis of the lubrication theory, we demonstrate the existence of significant transient growths in the parameter space region where the dynamical system is asymptotically stable, and show how they depend on the main physical parameters. In particular, the key role of the density ratio is highlighted.

DOI: 10.1103/PhysRevE.80.036312 PACS number(s): 47.15.Fe, 47.20.Ma, 47.27.nd, 47.50.−d

I. INTRODUCTION

In this work, we study interfacial instability in two superposed layers of power-law fluids focusing on non-normality and transient behavior of the dynamical system. The problem of interfacial instability is relevant in chemical engineering, where layered flows are involved in many extrusion, transport, or coating processes such as the manufacturing of photographic emulsion plates [1]. Superposed non-Newtonian fluid layers are also studied in glaciology: ice is considered as a power-law fluid, sliding over a much less viscous mud layer [2,3]. Balmforth *et al.* [1] examined the stability of two superposed Newtonian and non-Newtonian fluid layers from the point of view of the asymptotic stability (i.e., when time tends to infinity) and defined the stability region in the parameter space. Although this kind of analysis is a powerful tool to investigate many fluid dynamical problems [4,5], the evolution of the system cannot be fully explained through eigenvalues [6–8]. Eigenvalue analysis in fact allows one to understand when small disturbances of the basic state decay to zero for long periods of time, but it is unable to predict whether disturbances decay monotonically or grow until they reach a maximum after which they follow their own asymptotic fate. Therefore, possible transient growths cannot be detected by classical eigenvalue analysis. This is a key point, since the occurrence of a transient growth can be important for several reasons. First, it implies that the system temporarily exhibits a very different evolution from that predicted by the eigenvalues. Second, the transient growth can be so remarkable to trigger nonlinear instabilities, in other words, disturbances amplify so much that they make nonlinear terms significant (the so-called by-pass transition [9,10]). Therefore, the system can result nonlinearly unstable although the eigenvalue analysis predicts a disturbance decay. Third, transient growth can occur at time scales that are comparable with those of observation of the process; it follows that one could judge the basic state unstable although the disturbances decay on much longer time scales than those of interest.

The previous points explain why transient growths have attracted much interest in fluid mechanics [6,11–15], where non-normality analysis has also been applied (e.g., see [5,8,16]). From a mathematical point of view, the existence of transient growths of a disturbance is in fact related to the degree of non-normality of the eigenvectors of the operator that describes the dynamics of the disturbances. In spite of this growing interest, only a few papers have dealt with non-normality in open-channel flows, i.e., where free surface is present (e.g., [17,18]).

In this setting, we study the transient behavior of a system formed of two superposed layers of power-law fluids. In the following section, the model developed by Balmforth *et al.* [1] is recalled and some results concerning the asymptotic stability are also shown. In the third section, non-normality and transient behavior are investigated in the region of the parameter space which has been classified as asymptotically stable. To this aim, the condition number, the pseudospectra (with some related quantities), and the growth function are obtained and discussed. Finally, some conclusions are drawn in the fourth section.

II. PROBLEM FORMULATION

Let us consider two superposed layers of incompressible and immiscible fluids flowing down an inclined plane. A Cartesian coordinate system is fixed, as shown in Fig. 1. The properties of the two fluid layers are, in general, different; therefore, we refer to the upper and lower layers using the

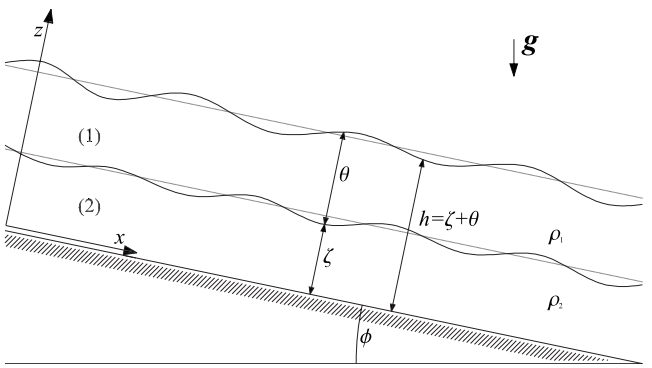

FIG. 1. Scheme of the physical problem investigated and main variables involved.

*carlo.camporeale@polito.it

subscripts 1 and 2, respectively. The two fluids have densities ρ_1 and ρ_2. The lower layer has a thickness $\zeta(x,t)$ (where t is time) and the upper layer has a depth $\theta(x,t)$, thus the composite layer has a thickness $h(x,t)=\zeta(x,t)+\theta(x,t)$. The flow is described by the two-dimensional velocity field $\{u(x,z,t),w(x,z,t)\}$ and the pressure $p(x,z,t)$. Surface tension is neglected both on the free surface and on the dividing interface.

The governing equations for both layers are the conservation of momentum and the continuity equation

$$\rho_j\left(\frac{\partial u}{\partial t}+u\frac{\partial u}{\partial x}+w\frac{\partial u}{\partial z}\right)=-\frac{\partial p}{\partial x}+\left(\frac{\partial \tau_{xx}}{\partial x}+\frac{\partial \tau_{xz}}{\partial z}\right)+\rho_j g_x \quad (1)$$

$$\rho_j\left(\frac{\partial w}{\partial t}+u\frac{\partial w}{\partial x}+w\frac{\partial w}{\partial z}\right)=-\frac{\partial p}{\partial z}+\left(\frac{\partial \tau_{xz}}{\partial x}+\frac{\partial \tau_{zz}}{\partial z}\right)-\rho_j g_z \quad (2)$$

$$\frac{\partial u}{\partial x}+\frac{\partial w}{\partial z}=0, \quad (3)$$

where $j=1,2$. In Eqs. (1) and (2), $\mathbf{g}=(g\sin\phi,-g\cos\phi)$ is the gravitational acceleration, and τ_{lm} are the components of the deviatoric stress tensor, the total tensor being $\mathbf{T}=\tau-p\mathbf{I}$.

A power-law rheology is adopted

$$\tau_{kl}=K_j\dot{\gamma}^{n_j-1}\dot{\gamma}_{kl}\equiv\mu_j(\dot{\gamma})\dot{\gamma}_{kl}, \quad (4)$$

where

$$\dot{\gamma}_{kl}\equiv\begin{pmatrix}2\frac{\partial u}{\partial x} & \frac{\partial u}{\partial z}+\frac{\partial w}{\partial x}\\ \frac{\partial u}{\partial z}+\frac{\partial w}{\partial x} & 2\frac{\partial w}{\partial z}\end{pmatrix},\quad \dot{\gamma}=\sqrt{\frac{1}{2}\dot{\gamma}_{kl}\dot{\gamma}_{lk}}. \quad (5)$$

The rheology in each layer is characterized by the consistency, K_j, and a power-law index, n_j. The effective viscosity is indicated by $\mu(\dot{\gamma})$. If $n_j=1$ for $j=1$ or $j=2$, then fluid 1 or 2 is Newtonian.

Nondimensionalization of Eqs. (1)–(3) is then performed. The variables of the problem, in a dimensionless form, are

$$x=L\tilde{x},\quad z=H\tilde{z},\quad u=U\tilde{u},\quad w=\frac{UH\tilde{w}}{L},\quad t=\frac{L\tilde{t}}{U} \quad (6)$$

with H the characteristic thickness of the composite, L the scale of the downslope lengths, and $U=(\rho g H^{2+n_2}\cos\phi/K_2L)^{1/n_2}$ the scale of fluid velocity. The Reynolds number,

$$\mathrm{Re}=\frac{\rho_1 UL}{K_2\left(\frac{U}{H}\right)^{n_2-1}}, \quad (7)$$

is considered in the zero limit and the hypothesis of the lubrication theory is introduced, i.e., $\epsilon=H/L\ll 1$ [1]. Some meaningful parameters are introduced: $D=\rho_2/\rho_1$ is the density ratio, $S=(L/H)\tan\phi$ is the slope parameter—which is of order one on the assumption of a gentle inclination of the inclined plane—while $R=(K_2/K_1)(U/H)^{n_2-n_1}$ is a ratio of dimensional, effective viscosities. The dimensionless equations governing the flow can therefore be written as (see Appendix A)

$$\frac{\partial\theta}{\partial t}+R^{1/n_1}\frac{\partial}{\partial x}\left[\frac{n_1\tau_I^{1/n_1}\theta^2}{2n_1+1}\right]+\frac{n_2}{n_2+1}\frac{\partial}{\partial x}\left[\frac{\theta}{\Delta_x}(\tau_B^{1+1/n_2}-\tau_I^{1+1/n_2})\right]=0 \quad (8)$$

$$\frac{\partial\zeta}{\partial t}+\frac{n_2}{n_2+1}\frac{\partial}{\partial x}\left[\frac{\zeta\tau_B^{1+1/n_2}}{\Delta_x}+\frac{n_2}{2n_2+1}\frac{1}{\Delta_x^2}(\tau_I^{2+1/n_2}-\tau_B^{2+1/n_2})\right]=0 \quad (9)$$

with $\tau_I=(S-\frac{\partial h}{\partial x})\theta$, $\tau_B=\tau_I+\Delta_x\zeta$, and $\Delta_x=SD-\frac{\partial\theta}{\partial x}-D\frac{\partial\zeta}{\partial x}$.

With regard to the classical stability analysis, Eqs. (8) and (9) were first linearized around the steady flow solution with a flat interface and free surface: $\zeta=Z$, $\theta=\Theta$, and $h=\Theta+Z=1$. A Fourier transform, in space and time, of the equations was then taken and, finally, the dispersion relation has been obtained. A region of asymptotic instability in the (k,R)-plane has been identified, through the eigenvalue analysis (see the example shown in Fig. 2). This region is generally contained in the $R<1$ half-plane (slight changes occur according to the layers thickness or rheology) (e.g., [1]). The values of the parameters connected to the points of the (k,R) plane outside the instability region define *asymptotically stable* flows. On the basis of these results, in the next section, we will examine whether these asymptotically stable configurations can experience transient growth of disturbances at finite times.

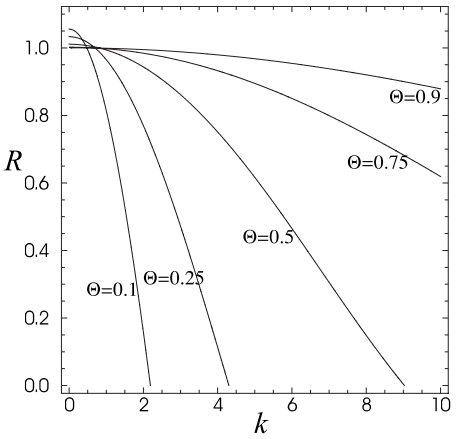

FIG. 2. Curves of neutral stability on the (k,R) plane for $S=1$, $D=1.1$, and $n_1=n_2=1$. The equilibrium flow is unstable below these curves.

III. NON-NORMALITY ANALYSIS

In order to investigate the non-normality of the dynamical system described by Eqs. (8) and (9), let us assume the solution in the normal-mode form

$$[\zeta(x,t),\theta(x,t)]=(Z,\Theta)+\{[\hat{\zeta}(t),\hat{\theta}(t)]e^{ikx}\}+\text{c.c.} \quad (10)$$

After substituting Eq. (10), Eqs. (8) and (9) are expanded into power series of $\hat{\zeta}$ and $\hat{\theta}$ and only first-order terms are

considered, thus linearizing the problem. The problem can then be restated in the following form

$$\frac{d\hat{\mathbf{q}}}{dt} = \mathbf{A}\hat{\mathbf{q}} \tag{11}$$

with $\hat{\mathbf{q}}=[\hat{\zeta}(t),\hat{\theta}(t)]$, $\mathbf{A}=\{a_{ij}\}\in\mathbb{C}^{2\times 2}$, and $a_{ij}=f(Z,\Theta,S,D,n_1,n_2,R)$ (the expressions of a_{ij} are reported in the Appendix B). We recall that Eq. (11) is valid in the zero Reynolds number limit. By assuming a dependence on time for $\hat{\mathbf{q}}$ in the form $e^{\lambda t}$, the system (11) can be restated as an eigenvalue problem whose solution gives the eigenvalues λ of $\mathbf{A}$ used in asymptotic stability analysis.

A. Disturbance energy

In order to quantify the transient growth of the disturbance, it is necessary to define the energy of the fluctuations of the steady flow solution [17,5]. The kinetic-energy density in the wave-number space can be expressed as [17]

$$\hat{E}_c = \int_0^{Z+\Theta} \frac{|\hat{u}|^2}{2} dz. \tag{12}$$

As far as the potential energy is concerned, stratification of the fluid layers must be taken into account. To do this, we can imagine that the upper layer consists of a fluid with a density ρ_1, while the lower layer can be regarded as made up of two superposed layers of densities ρ_1 and $\Delta\rho=\rho_2-\rho_1$, respectively. The potential-energy density in the wave-number space, associated with the perturbation of the free surface, can therefore be expressed as

$$\hat{E}_{p,sur} = \frac{\cos\phi}{F^2}\frac{|\hat{\zeta}+\hat{\theta}|^2}{2} \tag{13}$$

with $F=U_s/\sqrt{gH}$ the free-surface Froude number and U_s the surface velocity.

For the perturbed interface, introducing $\Delta\rho$ instead of ρ_1 and recalling that $D=\rho_2/\rho_1$, we obtain

$$\hat{E}_{p,int} = (D-1)\frac{\cos\phi}{F^2}\frac{|\hat{\zeta}|^2}{2}, \tag{14}$$

where, given the gentle inclination of the bottom plane, we can assume $\cos\phi\approx 1$.

The total energy density in the wave-number space of the disturbance is therefore given by $\hat{E}_{tot}=\hat{E}_c+\hat{E}_{p,sur}+\hat{E}_{p,int}$. We now introduce the two-norm $\|\cdot\|_2$, defined by

$$\|\mathbf{x}\|_2 = (\Sigma|x_j|^2)^{1/2} \tag{15}$$

for a vector x and by

$$\|\mathbf{B}\|_2 = \max_{\mathbf{x}}\frac{\|\mathbf{Bx}\|_2}{\|\mathbf{x}\|_2} \tag{16}$$

for a matrix $\mathbf{B}$. We recall that adopting this kind of norm offers the advantage of using the powerful singular value decomposition technique, since the two-norm of a matrix is equal to its maximum singular value [19]. In the following equations, and in the next sections, the two-norm $\|\cdot\|_2$ will simply be denoted by $\|\cdot\|$. It is found that

$$\sqrt{\hat{E}_{tot}} = \|\mathbf{q}\| \tag{17}$$

if the vector $\mathbf{q}$ is defined as

$$\mathbf{q} = (q_1,q_2) = \{\alpha\hat{\zeta}(t)+\beta\hat{\theta}(t), \alpha^*\hat{\zeta}(t)-i\beta\hat{\theta}(t)\} \tag{18}$$

where

$$\alpha = \frac{1+i}{4b}\left(\sqrt{b(c^2+d^2)}+i\sqrt{b(4ab-c^2-d^2)}\right) \tag{19}$$

and the asterisk indicates the complex conjugate, while

$$\beta = \frac{(1+i)\sqrt{b}(c+id)}{2\sqrt{c^2+d^2}}, \tag{20}$$

with $\{a,b,c,d\}=f(Z,\Theta,S,D,n_1,n_2,R,\cos\phi/2F^2)$, (the expressions of a, b, c, and d are reported in Ref. [20]). System (11) can be recast as

$$\frac{d\mathbf{q}}{dt} = \mathbf{Bq} \tag{21}$$

where

$$\mathbf{B} = \mathbf{TAT}^{-1}, \quad \mathbf{T} = \begin{pmatrix} \alpha & \beta \\ \alpha^* & -i\beta \end{pmatrix}. \tag{22}$$

Equation (22) is a similarity transformation, hence matrices $\mathbf{A}$ and $\mathbf{B}$ have the same eigenvalues and the results of the spectral analysis of the previous work [1] do not lose validity. We also emphasize that the Froude number is proportional to Re and $\sin\phi$, therefore the original problem (11) formulated in the zero Reynolds number limit, with the assumption of small inclinations ϕ, requires keeping the Froude number small.

B. Investigation of the transient behavior

The spectral analysis developed by Balmforth and coworkers provides the region in the parameter space in which the system is asymptotically stable. Our investigation is focused on the effects of non-normality on the transient behavior in these regions to understand whether the problem admits transient growths.

1. Measure of the non-normality

It has been shown that the behavior of a physical system cannot be fully explained through eigenvalue analysis, in certain circumstances. This happens when we are examining problems for which the matrix of eigenvectors $\mathbf{V}$ is shown to satisfy the statement about the *condition number* of $\mathbf{V}$, $K(\mathbf{V})$, (see [8])

$$K(\mathbf{V}) = \|\mathbf{V}\|\|\mathbf{V}^{-1}\| \gg 1. \tag{23}$$

A matrix is defined as *normal* if it has a complete set of orthogonal eigenvectors. Generally speaking, $K(\mathbf{V})$ can vary in the range $[1,\infty)$ and the value $K(\mathbf{V})=1$ is possible if and only if $\mathbf{B}$ is normal, thus condition (23) means that matrix $\mathbf{B}$

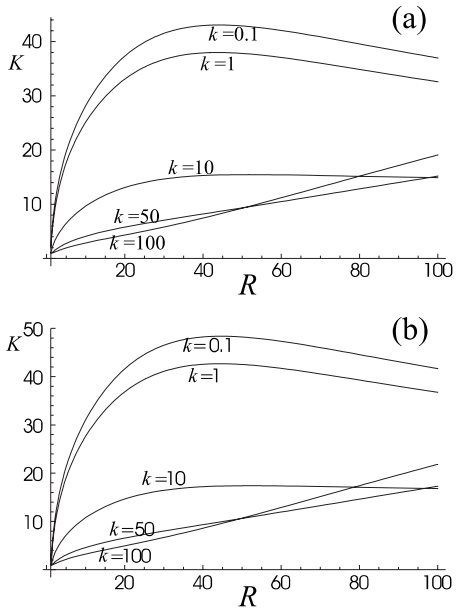

FIG. 3. Condition number versus viscosity ratio for different values of the wave number, with $S=1$, $D=1.025$, $Z=0.5$, $\Theta=0.5$, $n_1=1$, and $F=0.01$. (a) $n_2=1$, (b) $n_2=4/3$.

is *far* from being *normal*.

Figure 3 shows an example of the behavior of the condition number as a function of R. After several computations, we can observe that the condition number grows for small F, and a large density ratio or when $n_1<1$ or $n_2>1$, although the influence of fluid rheology is quite negligible [see Fig. 3(b)]. Finally, a large condition number can be found for thin lower layers. It is also found that the condition number is high for small wave numbers (i.e., for long waves) and for a growing viscosity ratio R, in particular for $R>1$, that is when the bottom fluid is the more viscous. Therefore, according to the condition number, non-normality is detected (and we can expect transient growth) for a large region in the parameter space.

2. Pseudospectra

Although the condition number is a simple and synthetic measure of non-normality, it is not so exhaustive in describing the transient behavior as it can overestimate the effects, so that more sophisticated tools are needed [8]. The general mathematical method consists of the examination of the pseudospectra and other important related quantities such as the numerical range and the numerical abscissa.

The ϵ-pseudospectrum σ_ϵ is the open subset of the complex plane, $z \in \mathbb{C}$, bounded by the ϵ^{-1} level curve of the norm of the resolvent, $\|(z\mathbf{I}-\mathbf{B})^{-1}\|$, where $\mathbf{I}$ is the identity matrix (see [8] for details and the algorithm). One can recognize the usefulness of the concept of pseudospectrum considering that, for a normal matrix, $\|(z\mathbf{I}-\mathbf{B})^{-1}\|$ is large when z is close to an eigenvalue of $\mathbf{B}$; for a non-normal matrix, $\|(z\mathbf{I}-\mathbf{B})^{-1}\|$ may be large even when z is far from the spectrum of $\mathbf{B}$. Furthermore, for a normal matrix, σ_ϵ is the union of circular disks centered on the eigenvalues and with a radius equal to ϵ, while, for a non-normal operator, involves a much larger set [8]. Limit values of pseudospectra give either the spectrum, $\sigma(\mathbf{B})$, when $\epsilon \to 0$, or the so-called *numerical range*, $W(\mathbf{B})$, when $\epsilon \to \infty$. The former is the set of eigenvalues, the latter is the set containing all the Rayleigh quotients of $\mathbf{B}$, i.e., $W \equiv \{\mathbf{x}^*\mathbf{B}\mathbf{x} : \mathbf{x} \in \mathbb{C}^N, \|\mathbf{x}\|=1\}$. Furthermore, the numerical abscissa, $\omega(\mathbf{B})$, is defined as the supremum of the real part of the numerical range of $\mathbf{B}$. It is known that the time derivative of the growth rate $\|e^{t\mathbf{B}}\|$ at $t=0$ is related to the numerical abscissa through the relation (see [8])

$$\left.\frac{d}{dt}\|e^{t\mathbf{B}}\|\right|_{t=0} = \omega(\mathbf{B}) = \sup \sigma\left(\frac{1}{2}(\mathbf{B}+\mathbf{B}^*)\right) \tag{24}$$

where $\mathbf{B}^*$ is the conjugate transpose of $\mathbf{B}$. An intrusion of the numerical range in the right half plane, i.e., when $\omega(\mathbf{B})>0$, indicates a transient growth. On the contrary, for normal operators, $W(\mathbf{B})$ is bounded by straight lines that cross the eigenvalues.

Figure 4 shows a computation example of the pseudospectra and the numerical range. Eigenvalues are also shown. The real parts of the eigenvalues are all negative, therefore an initial disturbance is expected to decay asymptotically to zero.

Non-normality of the operator is revealed by the fact that $\|(z\mathbf{I}-\mathbf{B})^{-1}\|$ is large, even when z is far from the spectrum. With respect to the numerical range, it is evident that it protrudes inside the right half plane, the numerical abscissa being positive, therefore transient growth is expected. If the

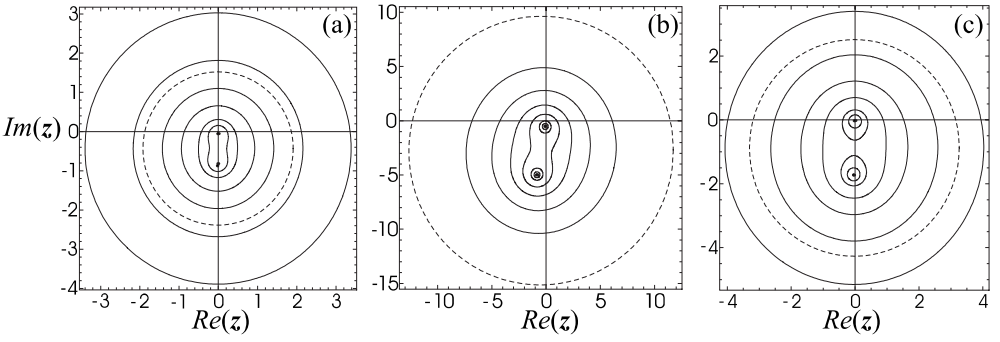

FIG. 4. Plot in the complex plane of spectra (dots), pseudospectra (solid lines), and numerical range (dashed line). The parameters of the contours from the inner to the outer are $\epsilon=[0.05,0.10,0.25,0.5,1,2]$. $S=1$, $D=1.025$, $n_2=1$, $F=0.01$, $k=0.1$, and $R=30$. (a) $n_1=1$, $Z=0.5$, (b) $n_1=4/3$, $Z=0.5$, (c) $n_1=1$, $Z=0.25$. Notice the different scales adopted in the panels.

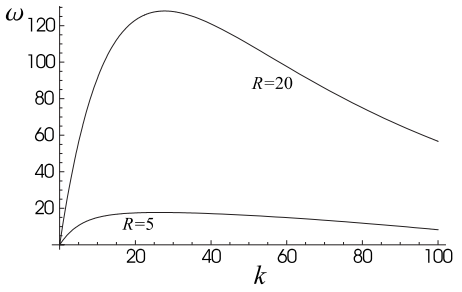

FIG. 5. The numerical abscissa versus the wave number for different values of the viscosity ratio, with $S=1$, $D=1.025$, $Z=0.5$, $\Theta=0.5$, $n_1=1$, $n_2=1$, and $F=0.01$.

size of a pseudospectrum is a measure of non-normality, we can see that non-normality is increased for small Froude numbers, for a density ratio which tends to 1, for rheology such that $n_1<1$ or $n_2>1$ and for a thicker lower layer than the upper one. Figure 5 shows an example of the behavior of the numerical abscissa. If $\omega(\mathbf{B})$ is positive, transient growth is expected, with an initial slope of the time-growth relation which depends on the magnitude of $\omega(\mathbf{B})$ itself. It has been observed that low Froude numbers, large values of R, thick lower layers or exponents satisfying $n_1 \leq 1$ or $n_2 \geq 1$ imply large intervals of wave-number values where transient growth may appear.

3. Growth function

In order to describe the transient growth, we now introduce the growth function, $\hat{G}(t)$, defined as the upper envelope of all possible evolutions, $G(t)$, of the normalized energy density, according to

$$\hat{G}(t) = \max[G(t)] = \max \frac{\|\mathbf{q}(t)\|^2}{\|\mathbf{q}_0\|^2} = \|\exp(\mathbf{B}t)\|^2 \qquad (25)$$

where $\mathbf{q}_0$ is the initial disturbance [8]. Figure 6 show some emblematic examples of the growth function. They refer to the case with the same basic thicknesses ($\Theta=Z=0.5$), slope parameter, S, equal to 1 and a Newtonian upper fluid (the other parameters, along with $\hat{G}_{max}$ and t_{max}, are listed in the Table I). The most evident feature is that the peak value of the growth function depends mainly on the density ratio and the Froude number: $\hat{G}_{max}$ increases when D tends to one and F is very low. For example, upper panels of Fig. 6 show that when the density ratio is very close to 1 and Froude number is 0.01, $\hat{G}$ can reach peak values of the order of 10^2 [e.g., see panel (a) where $\hat{G}_{max}=436$ at $t_{max}=11.26$]. Differently, the other parameters seem to play a minor role, even if values of $n_2>1$ promote slightly higher values of transient growth. Instead, with regard to the time t_{max} at which $\hat{G}_{max}$ is attained, we have observed that its order of magnitude is determined mainly by the wave-number k, while R, D, F, Z, and Θ have a less systematic impact: $\hat{G}_{max}$ is reached quickly for short waves. For both $\hat{G}_{max}$ and t_{max}, n_1 and n_2 seem almost irrelevant; this confirms that fluid rheology plays a not relevant role in inducing transient growths due to flow non-normality. Furthermore, we can appreciate the remarkable oscillatory structure of the temporal evolution. The period T is related to the frequency of the eigenvalues according to $T=2\pi/\mathrm{Im}(\lambda)$, where λ is the eigenvalue associated to the minimum growth rate. For example, in the cases shown in the six panels of Fig. 6 this estimate gives $T=19.5$, 1.15, 13.0, 32.7, 3.25, and 34.1, respectively, which is in good agreement with the values detectable from the figures.

IV. CONCLUSIONS

In this work, we have investigated the interfacial stability of superposed Newtonian and non-Newtonian fluid layers with the aim of detecting and quantifying transient growths. The condition number and the pseudospectra have revealed a significant non-normality of the linearized operator which describes the system, and different levels of non-normality have emerged, depending on the values of the different parameters. Remarkable transient growths have been detected in the zero Reynolds number limit and in regions of the parameter space where asymptotic exponential decay of perturbations is expected. Newtonian and non-Newtonian fluids

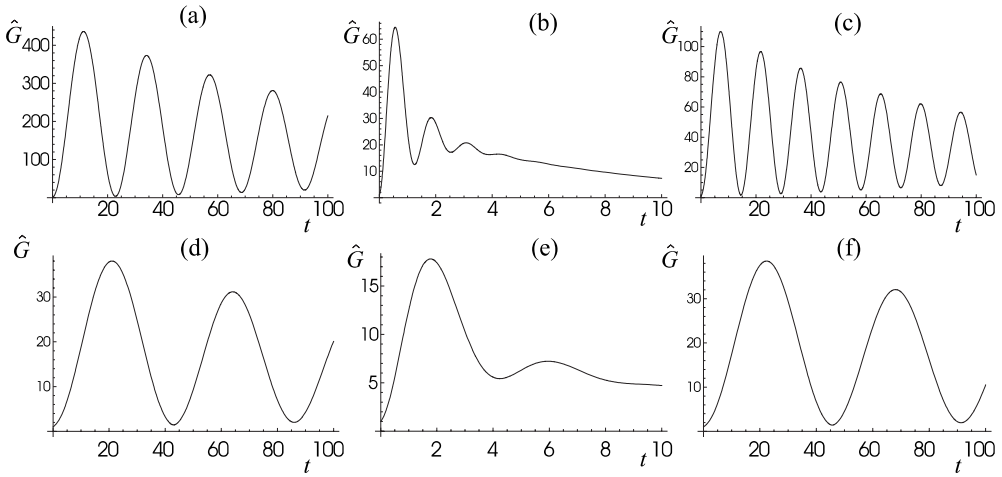

FIG. 6. The growth function versus time for some exemplifying parameter combinations (see Table I).

TABLE I. Parameters corresponding to the growth functions shown in the Fig. 6.

Case	S	Z	F	n_1	n_2	D	k	R	$\hat{G}_{max}$	t_{max}
(a)	1	0.5	0.01	1	1	1.005	0.1	10.3	436	11.26
(b)	1	0.5	0.01	1	1	1.025	1	19.3	64	0.56
(c)	1	0.5	0.01	1	4/3	1.025	0.1	16.8	110	7.17
(d)	1	0.5	0.1	1	1	1.025	0.1	5.0	38	21.0
(e)	1	0.5	0.1	1	1	1.025	1	5.1	18	1.77
(f)	1	0.5	0.1	1	4/3	1.025	0.1	4.8	39	22.37

have showed about the same behavior, demonstrating that fluid rheology is not the key variable in the investigated problem. On the contrary, the density ratio has proved to be the parameter which determines the magnitude of the transient growth to the greatest extent: as D tends to unity, $\hat{G}_{max}$ becomes increasingly large and values of the order of 10^2 can be attained. This tendency can be explained physically in the following way. In the case of asymptotically stable conditions, the perturbations of the basic state tend to disappear because of gravity that works to restore the state with minimum energy (i.e., a flat boundary between the fluids). Being this action by gravity proportional to the density difference, D, it follows that when $D \to 1$ the force driving the system towards the stratified equilibrium condition reduces and transient growths can develop.

ACKNOWLEDGMENTS

This work was partially supported by CRC (Cassa di Risparmio di Cuneo) and CRT (Cassa di Risparmio di Torino) Foundations.

APPENDIX A: DERIVATION OF Eqs. (8) and (9)

In this appendix the main passages in order to obtain Eqs. (8) and (9) are recalled [1]. The starting point are the Eqs. (1)–(3). The following boundary conditions are imposed

$$u(x,0,t) = w(x,0,t) = 0, \tag{A1}$$

$$u(x,\zeta^-,t) = u(x,\zeta^+,t) = u_I(x,t), \tag{A2}$$

and

$$w(x,\zeta^-,t) = w(x,\zeta^+,t) = w_I(x,t) = \frac{\partial \zeta}{\partial t} + u_I \frac{\partial \zeta}{\partial x}, \tag{A3}$$

where the subscript I refers to the interfacial velocities. Relation (A1) sets the no-slip condition on the inclined wall, while Eqs. (A2) and (A3) set the continuity of velocities and the kinematic condition on the interface, respectively. Moreover, the conditions

$$\mathbf{T}(x,\zeta^-,t) \cdot \begin{pmatrix} -\frac{\partial \zeta}{\partial x} \\ 1 \end{pmatrix} = \mathbf{T}(x,\zeta^+,t) \cdot \begin{pmatrix} -\frac{\partial \zeta}{\partial x} \\ 1 \end{pmatrix}, \tag{A4}$$

$$w(x,h,t) = \frac{\partial h}{\partial t} + u(x,h,t)\frac{\partial h}{\partial x}, \tag{A5}$$

and

$$\mathbf{T}(x,h,t) \cdot \begin{pmatrix} -\frac{\partial h}{\partial x} \\ 1 \end{pmatrix} = \mathbf{0}, \tag{A6}$$

are set. They impose the stress balance on the interface and the kinematic condition and stress continuity on the free surface at $z=h$, respectively.

It is assumed that the Reynolds number is smaller than one. Substituting Eq. (6) into Eqs. (4) and (5), one obtains

$$\tau_{kl} = K_2 \left(\frac{U}{H}\right)^{n_2} \tilde{\tau}_{kl}, \tag{A7}$$

where the dimensionless deviatoric stresses are expressed as

$$\tilde{\tau}_{kl} = \begin{cases} R^{-1} \dot{\gamma}^{(n_1-1)} \dot{\gamma}_{kl} & \zeta \le z \le h \\ \dot{\gamma}^{(n_2-1)} \dot{\gamma}_{kl} & 0 \le z \le \zeta \end{cases} \tag{A8}$$

with $R=(K_2/K_1)(U/H)^{n_2-n_1}$. The dimensionless equations describing the conservation of momentum and the continuity of flow are obtained by substituting Eqs. (6) and (A7) into Eqs. (1)–(3) (we drop the tilde superscript, all variables being dimensionless)

$$\epsilon^2 D_j \,\mathrm{Re}\left(\frac{\partial u}{\partial t} + u\frac{\partial u}{\partial x} + w\frac{\partial u}{\partial z}\right) = -\frac{\partial p}{\partial x} + \epsilon\frac{\partial \tau_{xx}}{\partial x} + \frac{\partial \tau_{xz}}{\partial z} + SD_j \tag{A9}$$

$$\epsilon^4 D_j \,\mathrm{Re}\left(\frac{\partial w}{\partial t} + u\frac{\partial w}{\partial x} + w\frac{\partial w}{\partial z}\right) = -\frac{\partial p}{\partial z} + \epsilon^2\frac{\partial \tau_{xz}}{\partial x} + \epsilon\frac{\partial \tau_{zz}}{\partial z} - D_j \tag{A10}$$

$$\frac{\partial u}{\partial x} + \frac{\partial w}{\partial z} = 0 \tag{A11}$$

with $D_j=\rho_j/\rho_1$, $S=(L/H)\tan\phi$, and $\epsilon=H/L$. The lubrication hypothesis is now introduced [1], namely, $\epsilon \ll 1$. The momentum Eqs. (A9) and (A10) become

$$0 = -\frac{\partial p}{\partial x} + \frac{\partial \tau_{xz}}{\partial z} + SD_j \tag{A12}$$

$$0 = -\frac{\partial p}{\partial z} - D_j. \tag{A13}$$

Equation (A13) is integrated and, subsequently, also Eq. (A12). Then, combining Eq. (A8) with the expression of τ_{xz}, one can write

$$\frac{\partial u}{\partial z} = \begin{cases} R^{1/n_1}\left(S - \dfrac{\partial h}{\partial x}\right)^{1/n_1}(h-z)^{1/n_1}, & \zeta < z < h \\ [\Delta_x(\zeta - z) + \tau_I]^{1/n_2}, & 0 < z < \zeta. \end{cases} \tag{A14}$$

Finally, the continuity equation is integrated over z. After imposing the conditions (A3), (A5), and (A1) and substituting the z derivative of u, Eq. (A14), we obtain

$$\frac{\partial \theta}{\partial t} + R^{1/n_1}\frac{\partial}{\partial x}\left[\frac{n_1 \tau_I^{1/n_1}\theta^2}{2n_1+1}\right] + \frac{n_2}{n_2+1}\partial_x\left[\frac{\theta}{\Delta_x}(\tau_B^{1+1/n_2} - \tau_I^{1+1/n_2})\right] = 0 \tag{A15}$$

$$\frac{\partial \zeta}{\partial t} + \frac{n_2}{n_2+1}\frac{\partial}{\partial x}\left[\frac{\zeta \tau_B^{1+1/n_2}}{\Delta_x} + \frac{n_2}{2n_2+1}\frac{1}{\Delta_x^2}(\tau_I^{2+1/n_2} - \tau_B^{2+1/n_2})\right] = 0, \tag{A16}$$

namely the differential Eqs. (8) and (9).

APPENDIX B: COEFFICIENTS OF MATRIX A IN THE MODEL (11)

In order to write the coefficients in a more compact form, we define the following quantities

$$\kappa = [S(DZ + \Theta)]^{1/n_2}, \quad \phi = (n_2 + 1), \tag{B1}$$

$$\delta = (2n_2 + 1), \quad \xi = (2n_1 + 1), \quad \omega = RS\Theta, \tag{B2}$$

and

$$\upsilon = [(D-1)SZ + S], \quad \psi = (S - SZ)^{1/n_2}. \tag{B3}$$

We can then write

$$a_{11} = \frac{k^2(D^2\phi Z^2\kappa - n_2\Theta^2\kappa + DZ\Theta\kappa + n_2\Theta^2\psi)}{D^2\phi\delta S} - ikZ\kappa,$$

$$a_{12} = \frac{k^2}{D^3\phi\delta S}[D^2 Z\kappa(n_2 Z + 2n_2\Theta + 1) + 2n_2^2\Theta^2\kappa - Dn_2\Theta\kappa(\delta\Theta + 2Z) + Dn_2\delta\Theta^2\psi - 2n_2^2\Theta^2\psi] - \frac{ik[DZ\kappa + n_2\Theta(\psi - \kappa)]}{D^2\phi},$$

$$a_{21} = \frac{k^2\Theta[\Theta(D\phi\omega^{1/n_1} - \xi\psi) + D\xi Z\kappa + \xi\Theta\kappa]}{D\xi\phi S} - ik\Theta\kappa,$$

$$a_{22} = \frac{k}{D^2\xi\phi S}\{[D^2 k\phi\Theta^2\omega^{1/n_1} + k\xi n_2\Theta^2(\psi - \kappa) + Dk\xi\Theta(n_2\Theta + 1)\kappa - Dk\xi\phi\Theta^2\psi] + i[D^2\xi\phi S\Theta\omega^{1/n_1} + D^2\xi n_2 SZ\kappa - D\xi\delta S\Theta(\psi - \kappa)]\}.$$

[1] N. J. Balmforth, R. V. Craster, and C. Toniolo, Phys. Fluids **15**, 3370 (2003).
[2] D. R. MacAyeal, J. Geophys. Res. **94**, 4071 (1989).
[3] H. Engelhardt, N. Humphrey, B. Kamb, and M. Fahnestock, Science **248**, 57 (1990).
[4] P. Drazin and W. Reid, *Hydrodinamic Stability* (Cambridge Univ. Press, Cambridge, 1981).
[5] P. J. Schmid and D. S. Henningson, *Stability and Transition in Shear Flows* (Springer-Verlag, New York, 2001).
[6] L. N. Trefethen, A. E. Trefethen, S. C. Reddy, and T. A. Driscoll, Science **261**, 578 (1993).
[7] P. J. Schmid, Annu. Rev. Fluid Mech. **39**, 129 (2007).
[8] L. N. Trefethen and M. Embree, *Spectra and Pseudospectra* (Princeton University Press, Princeton, 2005).
[9] D. Rempfer, Annu. Rev. Fluid Mech. **35**, 229 (2003).
[10] C. Lee and J. Wu, Appl. Mech. Rev. **61**, 030802 (2008).
[11] W. O. Criminale and P. G. Drazin, Stud. Appl. Math. **83**, 123 (1990).
[12] L. H. Gustavsson, J. Fluid Mech. **224**, 241 (1991).
[13] K. M. Butler and B. F. Farrel, Phys. Fluids A **4**, 1637 (1992).
[14] S. C. Reddy and D. S. Henningson, J. Fluid Mech. **252**, 209 (1993).
[15] S. V. Malik and A. P. Hooper, Phys. Fluids **19**, 052102 (2007).
[16] L. Boberg and U. Brosa, Z. Naturforsch., A: Phys. Sci. **43a**, 697 (1988).
[17] P. J. Olsson and D. S. Henningson, Stud. Appl. Math. **94**, 183 (1995).
[18] M. South and A. Hooper, J. Fluid Mech. **381**, 121 (1999).
[19] G. Golub and C. Van Loan, *Matrix Computations* (John Hopkins University Press, Baltimore, 1996).
[20] See EPAPS Document No. E-PLEEE8-80-050909 for expressions for a, b, c, and d in Eqs. (19) and (20). For more information on EPAPS, see http://www.aip.org/pubservs/epaps.html.